



# Resilience of standalone hybrid renewable energy systems: The role of storage capacity

Shoki Kosai <sup>a, b,\*</sup>, Jordi Cravioto <sup>c</sup>

<sup>a</sup> Department of Mechanical Engineering, College of Science and Engineering, Ritsumeikan University, Shiga, Japan

<sup>b</sup> Graduate School of Energy Science, Kyoto University, Kyoto, Japan

<sup>c</sup> Institute of Advanced Energy, Kyoto University, Kyoto, Japan



## ARTICLE INFO

### Article history:

Received 16 September 2019

Received in revised form

10 January 2020

Accepted 10 February 2020

Available online 13 February 2020

### Keywords:

Zero energy building

Sustainable rural living

Energy security

Redundancy

Vulnerability

Data envelopment analysis

## ABSTRACT

Evaluating the resilience of a power supply system after a sudden disturbance is essential in standalone hybrid renewable systems. Reliability assessments have strongly focused on the static condition during supply, opposite to the dynamic response to sudden disturbances, which is less studied in reliability literature. This study proposes a novel approach to analyze dynamic-response resilience from a sudden disturbance, focusing on the role of storage capacity of the standalone hybrid renewable system. Using a computer-based simulation, the magnitude, duration and instant of battery failure in the system is quantified and two indices to quantitatively measure resilience based on the three parameters are developed. Using these indices, it is discovered that the system resilience non-linearly declined with increasing trouble rate and trouble duration. The same tendency was observed for ten battery capacities analyzed. Also, larger storage capacity provided higher resilience as a general rule. However, battery capacities of 11,500, 12,500 and 14,500 Wh seem to equal or even slightly outperform the immediate larger type at the most critical duration and magnitude of failure. The developed algorithm presents one approach to clarify dynamic performance of the system and can be implemented in any system scale.

© 2020 Elsevier Ltd. All rights reserved.

## 1. Introduction

In recent decades, the acceleration of energy demand and fossil fuel depletion has drastically changed the global energy landscape. The use of renewables and local electricity production is increasingly being adopted in rural and urban communities. This shift has the potential to address several energy related issues such as more effective utilization of emerging technology, economic cost reduction, preservation of traditional schemes, and most importantly security of supply.

Renewable energy is a community-based type of energy, which is highly associated with the concept of local production for local consumption. The application of renewable energy has diverse advantages and disadvantages depending on the nature of the community where it is applied.

One of the most promising applications is among the least advantaged, namely rural communities which in most cases are segregated from the areas of higher economic development, and

which lack of support to connect with the centralized power infrastructure. Often, these groups realize that for electricity suppliers it is not worth investing in the extension of the existing electricity grid to a remote community having a small number of inhabitants [1]. In fact, 15% of the global population has no access to electricity [2], and conventionally they opt for more expensive, noisy and contaminating diesel-powered generation to produce electricity [3]. However, the utilization of diesel generators entails many risks, such as economic (e.g. expensive fuel cost), environmental (e.g. CO<sub>2</sub> emissions) and of security of supply (e.g. fossil fuel depletion).

Besides its applications in remote communities, in urban contexts there is a shift from centralized electricity supply to independent distributed micro grid and self-sustained small scale power supply systems, both utilizing renewable energy. The reasons for such shift are mainly economic and of environmental concern. Zero energy buildings (ZEB) and houses (ZEH) are one example of major solutions utilizing renewable energy technology [4,5], because ZEB and ZEH can self-supply themselves through a solar photovoltaic (PV) system installed on-site, for example, and also supply electricity to the grid [6]. Many countries have already initiated the concept of ZEB/ZEH as their future building energy

\* Corresponding author. Department of Mechanical Engineering, College of Science and Engineering, Ritsumeikan University, Shiga, Japan.

E-mail address: [kosai0203@gmail.com](mailto:kosai0203@gmail.com) (S. Kosai).

## Nomenclature

AM	Arithmetic mean
CO <sub>2</sub>	Carbon dioxide
CCR model	Chames, Cooper and Rhodes model
DEA	Data envelopment analysis
DMU	Decision making unit
DI curve	Duration-instant curve
EENS	Expected energy not supplied
GM	Geometric mean
HM	Harmonic mean
LOLE	Loss of load expectation
LOLP	Loss of load probability
LPSP	Loss of power supply probability
PV	Photovoltaic
RI curve	Rate-instant curve
RMS	Root mean square
SD	System dynamics
ZEB	Zero energy building
ZEH	Zero energy house

In contrast to the static nature of reliability, the dynamic condition of the power system has been simply dimmed out from the measurement of continuous power supply in the research topic on the hybrid renewable and storage system. The dynamic behavior of power system arises from the sudden disturbances. Particularly, in recent decades, the extreme events such as natural disasters (e.g. Hurricane Katrina in 2005, Great East Japan Earthquake in 2011, and Hurricane Sandy in 2012) exposed the vulnerable power system in ensuring continuous energy supply [40]. Not only the unavoidable natural disaster occurrence, but also the governmental action, social movement and legal request potentially triggered the sudden loss of power generation in the national grid [41]. These extreme sudden disturbances caused the extensive blackouts, having a critical impact on the society and the economy [42]. Therefore, it is of utmost importance to improve the power system ability to withstand the extreme sudden disturbance, called system resilience [43,44]. The resilient assessment can be utilized for the planning and designing of power system. Since resilience is an emerging concept in the power system narratives, some of research works addressing the low-probability extreme events [45], apparently associated with the resilience, were discussed in the reliability assessment (e.g. Refs. [46,47]).

In earlier research works of technical power system narratives, the resilience assessment has focused on the transmission and distribution lines [48] and the effectiveness of microgrids in the islanding mode to improve the resilient electricity line by preventions of cascading outage was widely highlighted [49–51]. Several probabilistic indices were applied to quantify the resilient including LOLP [46], EENS [46,47], Severity Risk Index (considering the probability and impact of failure scenario) [52], Resilience Achievement Worth Index (the upper limit on component sustained outage rate) [53]. However, the non-consideration of dynamic resilient assessment for determining the capacity size of hybrid renewable and storage system might be due to the complexity of computational modelling [54], high cost for the model simulation [54], theoretical barriers [39], and lack of sufficient data [55].

Notwithstanding the difficulties of taking into account the resilience assessment, limited research works incorporated the uncertainties along with the concept of resilience in the reliability assessment in the hybrid renewable and storage system. Chaudry et al. analyzed the impact of outage of various system components on the reliability of the national grid [56]. Javadian et al. integrated the outage factors including the duration and magnitude in the reliability assessment of distributed network [57]. Kosai et al. conducted the parametric analysis by changing the instant, duration and magnitude of sudden generator losses in the reliability and security assessment of the standalone microgrid [58] and individual house [59,60]. Meanwhile, the sudden disturbances on the storage facilities have been scarcely considered. It is widely accepted that the storage technology contributes to the improvement of power system resilience [11,61]. Storage technology is useful for the dynamic and quick response of power flow [62] is flexible for charging in the microgrids restoration [63]. Given the important role of storage technology in terms of system resilience, it is of significant importance to assess the impact of sudden losses of storage capacity on the continuous power supply in the hybrid renewable and storage system. Newer analyses need to focus on the separation between the static reliability and the dynamic resilience and the analysis of sudden occurrence of disturbance in storage technology might be suitable for such purpose. In addition, depending on the approach taken, outcomes might also be used in power supply planning.

Therefore the objective of this paper is to establish a methodology for analyzing the power system resilience in response to the

target. For instance, the United States has set a zero-energy target of 50% for commercial buildings by 2040 and a net zero target for all commercial buildings by 2050 [7]. Other countries have also set their own targets.

Given the stochastic and intermittent characteristics of renewables, the installation of storage technology in the hybrid renewable energy system is of significant importance. In spite of drawbacks of storage technology (e.g. the capital and maintenance costs and unavoidable energy losses through the round-conversion process [8,9]), the process of storage technology charging and discharging contributes to the power and load levelling and maintains the power stability [10]. Particularly, the standalone mode of power system requires the storage technology to store the excess energy produced by renewables so that it can play a role of energy source to meet the demand when the demand surpass the power from renewables. The contribution of storage technology to the continuous electricity supply cannot be simply ignored [11].

In order to ensure the security of power supply, many research works have conducted reliability assessments of a hybrid renewable and storage system. Reliability is defined in the research area of power system as the measurement of the system ability to supply a desired amount of power to the end-users within a specific standard [12,13]. The system reliability is quantified through the implementation of computing various indices including Loss of Power Supply Probability (LPSP) [14–21], Loss of Load Expectation (LOLE) [22], Loss of Load Probability (LOLP) [23–28], and Expected Energy Not Supplied (EENS) [29]. These reliability indices were developed on a basis of probabilistic model [30]. Most research works assessing the reliability of hybrid renewable and battery systems have considered the standalone microgrids in a remote area. Meanwhile, several research works focused on the grid-connected microgrids with storage technology [31,32] or without it [33,34] in urban areas. In order to determine the optimal capacity size of renewable energy and storage technology, the reliability was also assessed in the individual ZEB/ZEH [35–37].

It must be noted that almost all research inadvertently have focused on the long-term static condition in the reliability assessment. In most investigations no mention is given to the distinction between the short-term and long-term condition of their assessment. Only few works have pointed out the difference [38,39]. And these have not approached the short-term one.

sudden disturbances of storage technology and to identify the optimal capacity size, focusing on the standalone hybrid renewable and storage system.

This article is structured as follows. Section 2 develops the methodology of analyzing the system resilience taking into consideration the sudden disturbances of storage technology. Section 3 introduces the case study for applying the methodology. The quantified resilience of power system against the sudden disturbances and the optimal capacity size are presented in Section 4. Finally, Section 5 summarizes the conclusions.

## 2. Methodology

The system resilience will be quantified in the parametric approach and then the optimal capacity size will be determined based on a multi-variable comparative efficiency indicator developed using data envelopment analysis (DEA).

### 2.1. Quantification of system resilience

#### 2.1.1. Concept of sudden disturbances on storage technologies

In the time-scale form, threats to the security of electricity in the power system is categorized into a short-term episodic shock and long-term secular stress [64]. The long-term secular stress is a static vulnerability of power system (e.g., environmental burden, depletion of fuels, growth of power demand) [65]. Meanwhile, the short-term episodic shock is a dynamic vulnerability of power system and occur unexpectedly at a given instant [89], which is referred to sudden disturbances in this study.

The core analysis of this article corresponds to assessing system resilience, i.e. the ability of standalone power system to remain self-sufficient after the occurrence of sudden disturbances with the storage technology. Batteries represent the storage technology in this paper. The cause of fail might be burning due to the heat generation of module, short circuit, initial failure due to human errors, and the use of electric appliances requiring a significant starting voltage and power consumption with connecting to specific loads. The concept of *battery trouble* needs structuring based on the three factors: “battery trouble rate”, “battery trouble duration” and “instant of battery trouble”. These are defined as follows:

1. “Battery trouble rate” refers to the magnitude of the battery failure. It is parametrically set in the range of 0%–100%. For example, battery trouble rate is 0% when the battery is fully capable, and it rises to 100% if all parallel circuits within the battery fail.
2. “Battery trouble duration” represents the period that a battery failure lasts. It is measured in a time scale.
3. “Instant of battery trouble” stands for the time when the battery failure occurs. It is a specific time.

These three factors represented graphically in Fig. 1 are considered major parameters for evaluation of the system resilience of the standalone power system. With the sudden occurrence of battery trouble, the rate is instantly increased, remaining at the same level until recovery. Trouble duration in this research is less than 24 h in order to limit the time scale up to one day after sudden disruption. This is in accordance with the concept of short-term power reliability. The model is simulated by changing the three major parameters described above.

#### 2.1.2. Evaluation of accepted trouble rate and duration at the different instant of trouble

As outlined previously, trouble rate, trouble duration, and instant of trouble in the system batteries are the constituent

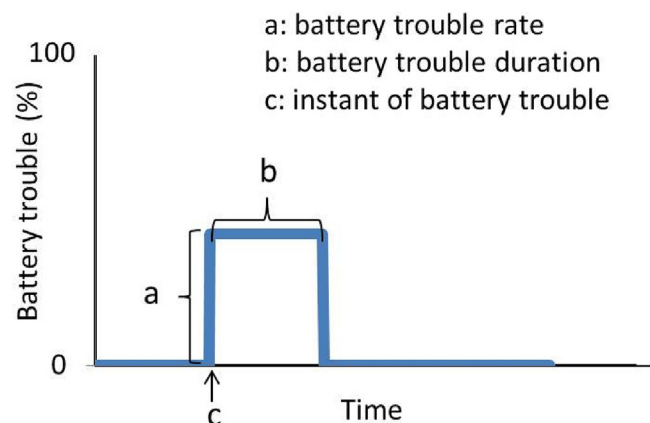


**Fig. 1.** Concept of sudden disturbances on storage technologies.

parameters for evaluation of system resilience. Particularly, both the maximum battery trouble rate and the maximum battery trouble duration corresponding to the different instant of battery trouble determine the ability of power system to remain self-sufficient. As an initial step variation in such parameters must be represented in order to generate the proposed indices of system resilience.

The first relationship represented is that between trouble duration and instant of trouble evaluated at different trouble rates. In this case, the focus is on the time duration when the standalone system remains self-sufficient. This relationship expressed graphically is known as the trouble duration-instant of trouble curve (hereafter, referred to DI curve). Such curve is obtained by changing the parameters in the steps, presented in Fig. 2. The mathematical expression representing the DI curve is the following:

$$DI\ curve = \max(\text{accepted trouble duration})_i \quad (1)$$

The second relationship under study is that between trouble rate and instant of trouble at different trouble duration. In this case, the focus is on the trouble rate at which the standalone electricity system remains self-sufficient. This relationship expressed graphically is known as the trouble rate-instant of time curve (hereafter referred to RI curve). Such curve is obtained by changing the parameters, presented in Fig. 3. The mathematical expression representing the RI curve is the following:

$$RI\ curve = \max(\text{accepted trouble rate})_i \quad (2)$$

The detail steps and definition of both DI curve and RI curve are presented in Appendix A.

Failures of power source components would be sudden disturbances, occurring in the flow of time. Addressing sudden disturbances generally refers to the evaluation of power systems under dynamic conditions [66]. In this study, sudden disturbances are parametrically induced in the system model, so the obtained outcomes indicate the dynamic behavior of the power system to some extent.

#### 2.1.3. Assessment of system resilience

To analyze system resilience in a quantitative manner this research proposes the two indices dedicated for system resilience based on the relations identified above:

1. Total accepted trouble duration throughout one-day.
2. Total accepted trouble rate throughout one-day.

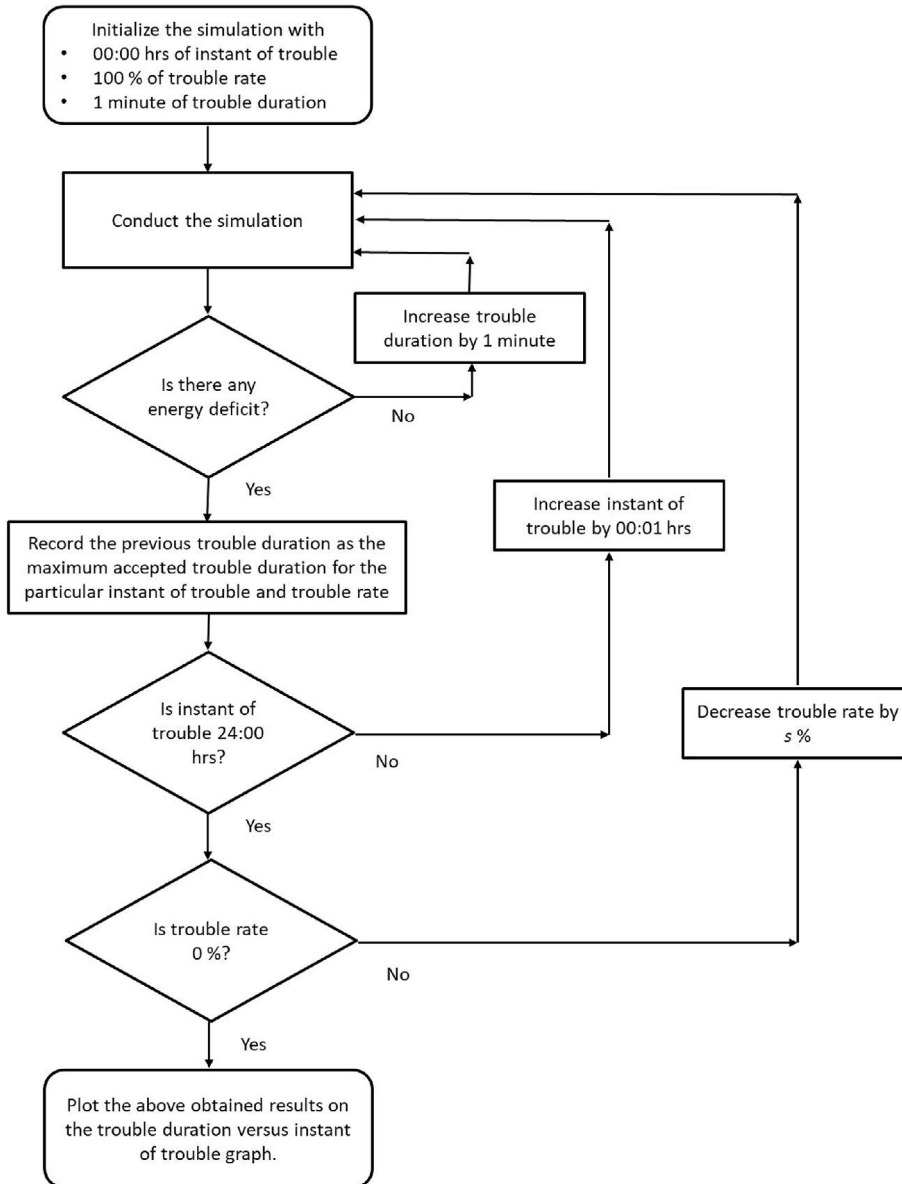


**Fig. 2.** Flowchart of the steps for obtaining the DI curve.

The concepts above are related to each of the plots obtained in through the methods detailed in the previous section. By calculating the “area under the curve” of these curves, using equations (3) and (4), the accepted trouble duration at the different trouble rate and the accepted trouble rate at the different trouble duration can be obtained.

$$\text{Resilience}_{DIx} = \int_{00:00}^{24:00} f_x(i) dt \quad (3)$$

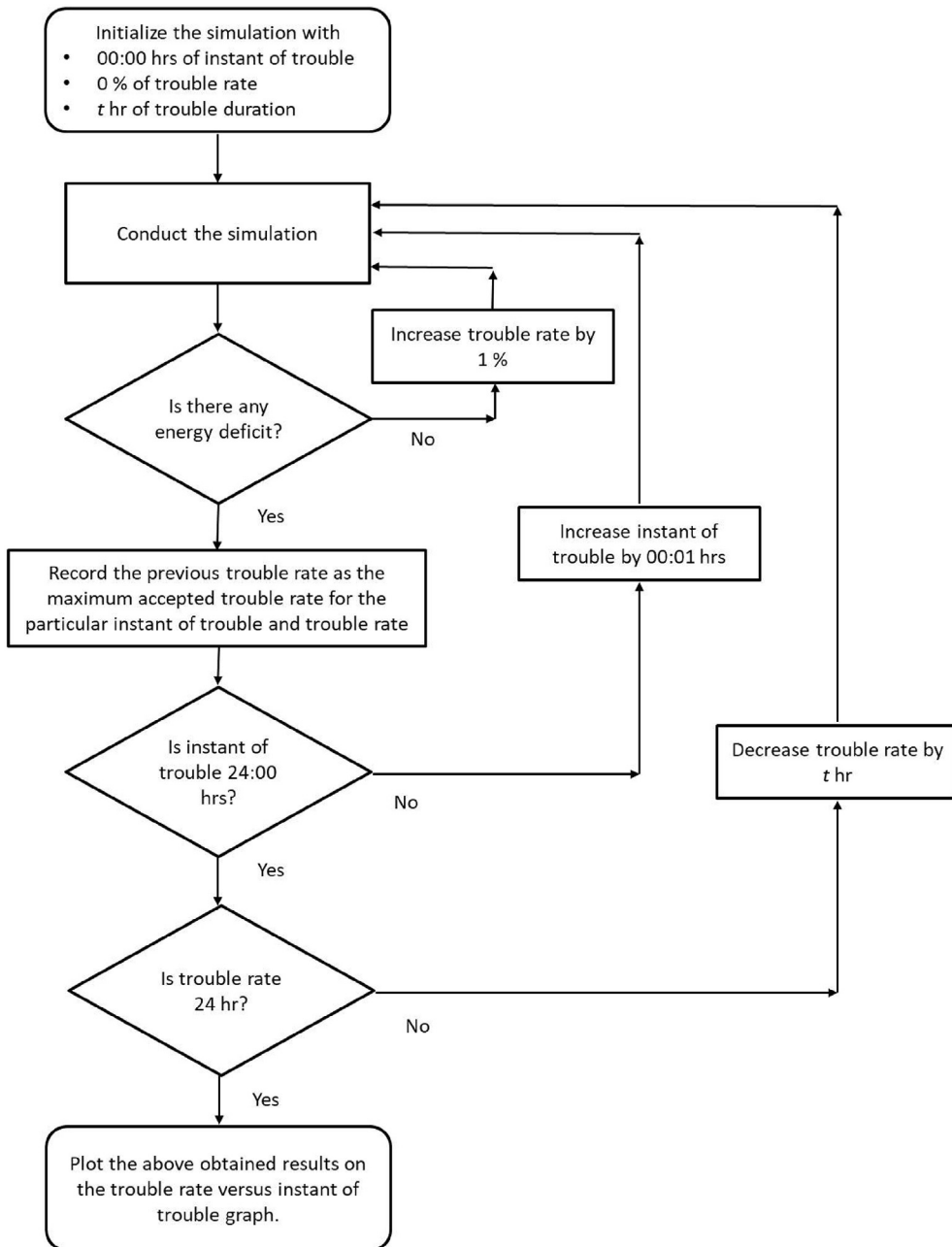
$$\text{Resilience}_{RIy} = \int_{00:00}^{24:00} g_y(i) dt \quad (4)$$

where,  $f(i)$ : DI curve,  $g(i)$ : RI curve,  $i$ : instant of trouble,  $x$ : battery trouble rate,  $y$ : battery trouble duration.

Finally, the accepted maximum component under the various

trouble rate and trouble duration needs to be synthesized into a composite overall resilience index. Here, two indices based on DI curve and RI curve are presented. Probability of magnitude and duration in battery trouble occurrence would determine the weighting for each of rate options and of duration options. Given that their probabilities randomly vary depending on the custom service quality, location and instant of time, for simplicity, this paper assigns the equal weight for each of rate options and of duration options. Each of accepted trouble duration and accepted trouble rate under the various options are respectively aggregated to obtain the resilience indices by using the technique of root mean square in the following equations.

$$\text{Overall Resilience}_{DI} = \sqrt{\frac{\sum \text{Resilience}_{DIx}^2}{X}} \quad (5)$$

**Fig. 3.** Flowchart of the steps for obtaining the RI curve.

$$X = \frac{100}{s} + 1 \quad (6)$$

$$\text{Overall Resilience}_{RI} = \sqrt{\frac{\sum \text{Resilience}_{RI_y}^2}{X}} \quad (7)$$

$$Y = \frac{24}{t} + 1 \quad (8)$$

where, X: the number of assessed trouble duration options, Y: the number of assessed trouble rate options, s: interval of assessed trouble rate, t: interval of assessed trouble duration.

As a result, each component associates with system resilience

from the perspectives of trouble rate and trouble duration. The greater index corresponds to the stronger component of system resilience.

## 2.2. Optimal storage technology among standalone hybrid renewable energy systems

To determine the most resilient storage technology in the standalone hybrid renewable energy system, a comparison of the diverse systems is done using Data Envelopment Analysis (DEA). This comparison is based on capacity size of the hybrid power system and its associated resilience indices obtained in the previous section.

DEA is a mathematical method from the field of operations research developed to compare performance among several

decision making units (DMU) [67], and the comparison is assessed in terms of efficiency for each DMU. One important advantage of DEA is that it can handle several indicators with diverse units. Indicators are introduced into the model as inputs or outputs based on the direction of its effect on the efficiency. A linear programming problem is generated with efficiency of the DMU under analysis subjected to the efficiencies of other DMUs, and by solving for each DMU, the resulting efficiencies range from 0 to 100%, which can be interpreted as a 'benchmark index' with respect to the best performing DMU. The general form of the model is shown in equation (9), where  $E_m$  is the efficiency of the  $m$ th DMU,  $v_i$  is the weight assigned to output  $y_i$  (outputs range from  $j$  to  $J$ , this last being the total number of outputs);  $u_i$  is the weight assigned to input  $x_i$  (inputs range from  $i$  to  $I$ , correspondingly  $I$  the total number of inputs); and the conditions  $v_j \geq 0$  and  $u_i \geq 0$  for weights to be natural numbers.

$$\max E_m = \frac{(Outputs)_m}{(Inputs)_m} = \frac{\sum_{j=1}^J (v_j y_j)_m}{\sum_{i=1}^I (u_i x_i)_m}$$

subject to

$$(9)$$

$$0 \leq \frac{\sum_{j=1}^J v_j y_j n}{\sum_{i=1}^I u_i x_i n} \leq 1, \quad n = 1, 2, N$$

$$u_{im}, v_{jm} \geq 0, \quad i = 1, 2, I, \quad j = 1, 2, J$$

In order to compare storage technology in standalone hybrid renewable energy systems, the specific DEA formulation is modelled through the relationship of the two resilience indices obtained in the previous section and the storage cost of the system. Both indices (accepted trouble duration at different trouble rates, and accepted trouble rate at different trouble durations) take the role of inputs given that the lower its magnitude the higher the effect on efficiency, whereas the cost takes the role of the output, given its opposite effect. It is noteworthy that various economic indicators have also been utilized for determining the optimal capacity of hybrid renewable power system. These include levelized cost of energy [15], total annualized cost of system [68], and net present value [69]. While these indicators are proper for a long-term assessment, resilience is highly associated with a shorter-term notion closer to installation capacity costs. As such, the capital cost is selected as our economic indicator in this analysis of storage technology.

The resulting DEA model using overall resilience<sub>DI</sub>, overall resilience<sub>RI</sub>, and capital cost is detailed in equation (10) for the first battery capacity.

$$\max E_1 = \frac{(Capital\ cost)_1}{(Overall\ resilience_{DI} + Overall\ resilience_{RI})_1}$$

subject to

$$0 \leq \frac{\sum_{j=1}^J (capital\ cost)_n}{\sum_{i=1}^I (Overall\ resilience_{DI} + Overall\ resilience_{RI})_n} \leq 1, \quad n = 1, 2, N$$

$$u_{i1}, v_{j1} \geq 0, \quad i = 1, 2, I, \quad j = 1, 2, J$$

$$(10)$$

In equation (10) the objective function is the efficiency between the overall resilience<sub>DI</sub>, the overall resilience<sub>RI</sub> and its capital cost.

The optimization tries to find the efficiency of the first battery capacity subjected to the efficiencies of the other capacities. Similar linear programs have to be modelled and solved for every battery capacity.

In addition, two other DEA configurations are estimated. These correspond to DEA models using overall resilience<sub>DI</sub> and overall resilience<sub>RI</sub> separately as the input, and capital cost as the output. With these additional models a comparison based on the configuration with multiple indices and simpler ones will take place. Equations (11) and (12) are the models for the first battery capacity and similarly to the DEA model in equation (8), these are part of multiple linear programs for every capacity size.

$$\max E_1 = \frac{(Capital\ cost)_1}{(Overall\ resilience_{DI})_1}$$

subject to

$$0 \leq \frac{\sum_{j=1}^J (capital\ cost)_n}{\sum_{i=1}^I (Overall\ resilience_{DI})_n} \leq 1, \quad n = 1, 2, N$$

$$u_{i1}, v_{j1} \geq 0, \quad i = 1, 2, I, \quad j = 1, 2, J$$

$$\max E_1 = \frac{(Capital\ cost)_1}{(Overall\ resilience_{RI})_1}$$

subject to

$$0 \leq \frac{\sum_{j=1}^J (capital\ cost)_n}{\sum_{i=1}^I (Overall\ resilience_{RI})_n} \leq 1, \quad n = 1, 2, N$$

$$u_{i1}, v_{j1} \geq 0, \quad i = 1, 2, I, \quad j = 1, 2, J$$

As a final note, the DEA formulation described above uses what is known in DEA related literature as the CCR DEA model [70]. Applied to our case study, this means that the comparative analysis assumes constant returns in the efficiency relation between cost and resilience. This is so as to set the most efficient benchmark in the least number of storage technology types possible, and not to assume specific details about the production function. This procedure is also applied in contemporary DEA literature [71].

### 3. Case study

#### 3.1. Scope of research

As mentioned in Section 1, there are various potential applications of storage technology with renewable energy depending on the scale of the standalone system. As a starting point and for simplicity, this paper focuses on the case of households making the standalone electricity system. Home electricity demand and supply would be the simplest analysis of renewable energy use and storage and as such is adopted by the authors. Taking an imaginary case of a standalone zero energy home (ZEH) as a starting point, the assessment of system resilience after the occurrence of a sudden power disruption can be applied to any real standalone electricity system. In addition, it is of interest to the authors to select Japan for the analysis of the standalone ZEH, given its potential in urban contexts [72], and the targets set by the Japanese government to promote it [73]. Therefore, this analysis is focused on the standalone ZEH in Japan.

### 3.2. Standalone electricity system modelling

System Dynamics (SD) is utilized to model the power flow in the standalone ZEH shown in Fig. 4. SD is a simulation method of non-linear flows used to evaluate the complex and uncertain forthcoming phenomena [74]. The model of power demand and supply flow using SD is following the methodology developed by one of the authors (e.g. Refs. [41,59,75]). In this methodology a computer-based power flow model is configured to make the simulations, and by means of a comparison between the simulation results and outcomes of a real grid, the model is validated [41]. Such validation is focused on analyses of small intervals of power flow time series, proving that the SD-based model is accurate/adequate [76]. In the current power flow system, based on high similarities with a previously validated system it is conceivable to apply SD for the matter of analysis. These similarities are found in terms of the close-loop configuration and the diversity of available energy sources [77,78].

As shown in Fig. 4, the standalone electricity system contains two supply elements: renewable energy and storage technology. Solar PV and battery correspond to renewable energy and storage technology respectively. Given the minimum maintenance and convenient portability, solar PV is suitable for standalone ZEH and the primary energy source for power production in ZEH [79]. "Feed-in-tariff" with a 10-year warranty sale of acquisition for solar PV power started in 2009 in Japan and it leads to a gradual increase in the number of households with the expiration of warranty periods after 2019. It is reported that most of those households shift the use of surplus power from selling to consuming with the use of battery as the most well-known storage method in Japan and it is expected that the rate of battery installation increases after 2019 [80]. Therefore, these two appliances including solar PV and battery in ZEH are selected in this study.

The summation of power produced by solar PV and battery is defined as power delivery. The power delivery is utilized to meet the demand of home electricity, and surplus power exceeding demand is automatically transferred to the battery for storage. The energy stored in the battery is discharged when the home electricity demand surpasses the power generated by solar PV. It is assumed that the solar PV stops its operation once the battery is fully charged. The maximum demand load curve in Japan [81] is utilized as the input for demand of home electricity in this study.

In this study, power generated by solar PV is computed based on various components including roof-top area, PV efficiency, radiation, and solar panel rate. The solar panel rate is the rate of solar panel area to roof-top area and greater solar panel rate increases the capacity of solar PV. The irradiation data is taken from the solar

irradiation data in Japan, focusing on the date of maximum load demand [82]. The average house area in Japan ( $140 \text{ m}^2$ ) is used as input of roof-top area, and 19% of the converting efficiency of crystalline silicon solar cells as input of PV efficiency [83]. In sum, the power generated by solar PV is computed using equation (13).

$$\begin{aligned} \text{"Solar PV"} = & \text{"Roof - top area"} \times \text{"PV efficiency"} \times \text{"radiation"} \\ & \times \text{"solar panel rate"} \end{aligned} \quad (13)$$

Additionally, the use of Li-ion battery is assumed in the model since it is the most common battery type for the small scale of power system. Thus, 92% is taken as the battery efficiency factor [84]. All variables with corresponding definitions and units are summarized in Table 1.

As for the resilience assessment, this paper sets the number of options for the assessed trouble rate and duration as follows. It is assumed that the battery cell is composed of five low parallel circuits and this paper assesses the trouble rate by 20%, which is used as input for the variable  $s$ . Following the trend of solar PV generation, the interval of trouble duration is set as 4 h, which is used as input for the variable  $t$ . In addition, as for the analysis of capacity size, the capital cost in 2016 for lithium-ion battery and solar PV is used [85,86].

### 3.3. Precondition of modelling

Before the system resilience analysis in response to the sudden battery failure, the appropriate range of capacity size of battery must be identified. This is done by changing the parameters of both solar panel rate and battery capacity in the simulation model. The rationale behind this is that the standalone electricity system must guarantee a continuous supply of sufficient power to meet load demand.

Given that this model runs simulation from 00:00 h, a certain amount of energy needs to be stored in the battery to keep on discharging until the solar PV starts its operation in the morning. The minimum required energy in the battery at 00:00 h is initially identified. Then, the required minimum solar panel rate and minimum battery capacity are identified by analyzing the energy deficit of the power system. In our analysis, energy deficit is referred to the total lack of power delivery to meet the one-day load demand.

The earlier research which one of the authors reported [59] has identified these components of the same ZEH this paper assesses here. Based on the earlier research, the precondition of modelling is determined as follows. As for solar PV capacity, 20% of the

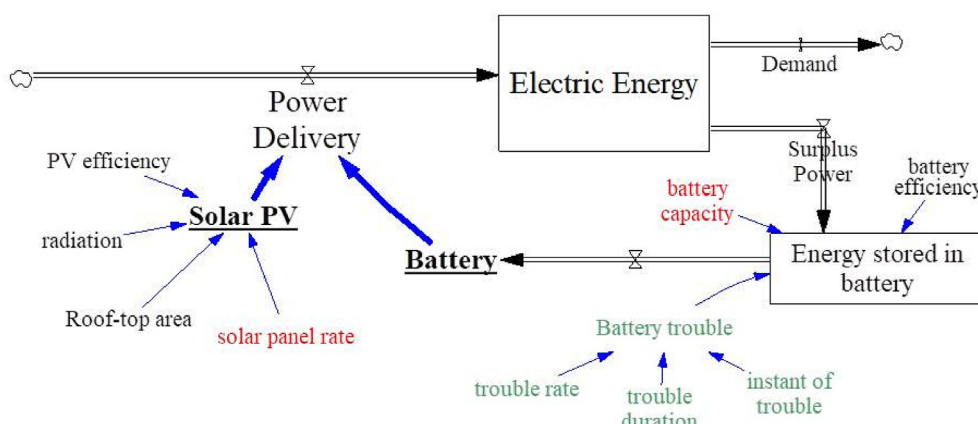


**Fig. 4.** Standalone electricity system model.

**Table 1**  
Definitions of variable.

Variable	Unit	Definition
Solar PV	W	Power generated by roof-top solar PV
PV efficiency	%	Conversion efficiency from solar irradiation to power
Radiation	W/m <sup>2</sup>	Solar irradiation
Roof-top area	m <sup>2</sup>	Home roof-top area
Solar panel rate	%	Rate of solar panel area to roof-top area
Power Delivery	W	Summation of power from solar PV and battery
Electric Energy	Wh	Imaginary energy differences between the sum of demand and surplus power, and power delivery
Demand	W	Load demand of home electricity
Surplus Power	W	Excess power not consumed by load demand
Energy stored in battery	Wh	Energy stored in battery
Battery efficiency	%	Battery round-trip efficiency
Battery capacity	Wh	Maximum energy stored in battery
Battery trouble	%	Sudden disruption of battery system
Trouble rate	%	Magnitude of battery trouble
Trouble duration	hr	Stoppage periods of battery operation
Instant of trouble	Hrs	Timing of battery trouble occurrence

minimum capacity margin is considered and 18% is used as input for the solar panel rate. Corresponding to the 18% of solar panel rate, 3740 Wh is used as input for the minimum required energy in the battery at 00:00 h. And then, given that 10,500 Wh is the required minimum battery capacity, this paper focuses on the 10 options in the range of almost 40% of the minimum capacity as follows: 10500 Wh, 11,000 Wh, 11500 Wh, 12,000 Wh, 12500 Wh, 13,000 Wh, 13500 Wh, 14,000 Wh, 14500 Wh, 15,000 Wh.

## 4. Results and discussion

### 4.1. DI and RI curves

The construction of the two plots necessary to evaluate system resilience described in section 2.1.2 yielded the DI curve and the RI curve. This Section demonstrates features of this process, using 13,000 Wh of battery capacity as the example.

First, the relationship between trouble duration and instant of trouble as seen through the DI curve (Fig. 5) shows that, in general, greater trouble rate observes less trouble duration at any instant of trouble. Based on this, the standalone electricity system will remain self-sufficient for a longer time with less rate of trouble, regardless of when it takes place.

Another interesting finding is that there is similar trend for any

trouble rate. This trend is described by a sharp decrease in trouble duration until the instant of trouble becomes 15:00, when it can drastically increase for trouble rates around 20%. If the trouble rate is higher than 20% this point of overshoot is delayed or shifted. The point of overshoot called time boundary in this article, sets a threshold from where system resilience can significantly improve. The occurrence of time boundary is due to that the system could be self-sustained and sustainable duration could be consequently extended as long as the battery could store a certain amount of energy to be used until the start of solar PV operation. Except for 100% of trouble rate, the time boundary is seen after 12:00 and with decreasing trouble rate it is seen in earlier hours. As also seen in Fig. 5, the time boundary observed for trouble rates of approximately 80–100% would occur during the morning. In these cases, any single moment of battery failure causes the supply disruption before the time boundary.

The RI curve (Fig. 6), in turn, shows that the trouble rate is higher with decreasing trouble duration, regardless of the moment when the trouble happens, as pointed out in Fig. 5, due to the inverse proportion between accepted trouble rate and trouble duration. Only in the case that trouble rate is less than 19%, the standalone system remains self-sufficient at any trouble duration.

It is noteworthy that the trend of this curve changes by length of trouble duration. In the cases of 4 h and 8 h, the accepted trouble

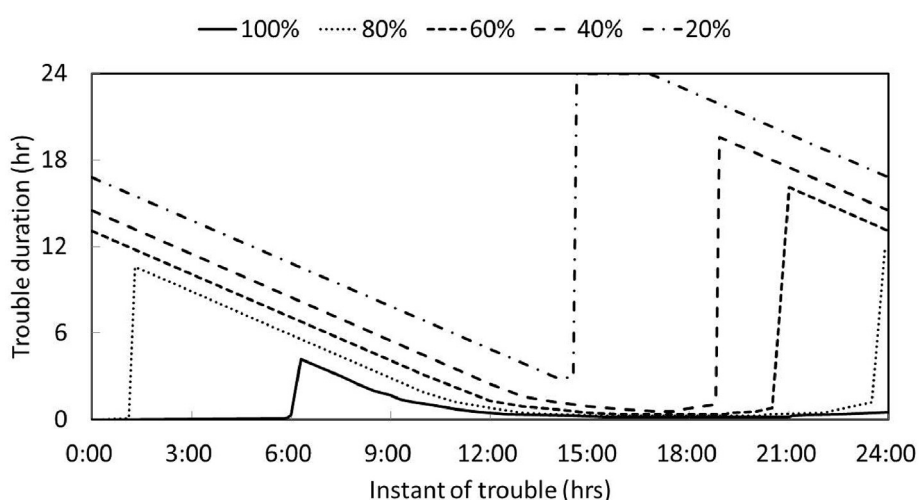


**Fig. 5.** Relation between trouble duration and instant of trouble at different trouble rates in the case of 13,000 Wh of battery capacity.

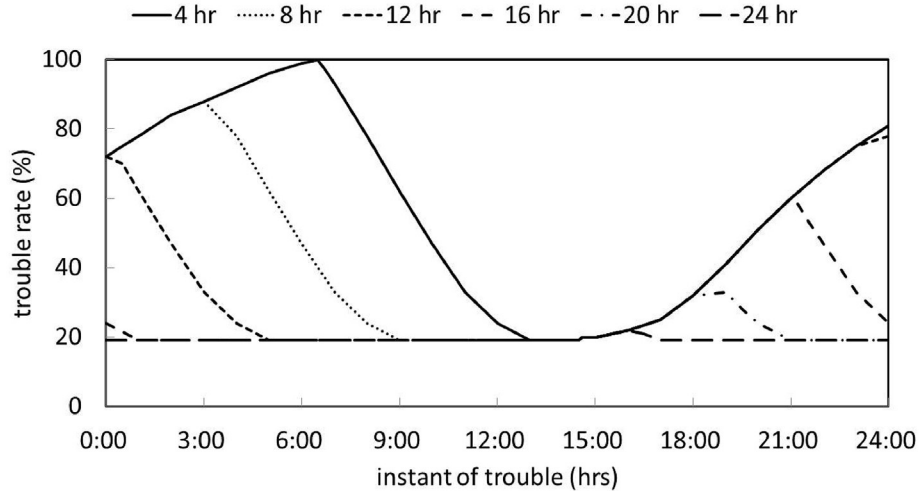


**Fig. 6.** Relation between trouble rate and instant of trouble at different trouble duration in the case of 13,000 Wh of battery capacity.

rate increases with time. It starts declining after reaching their peaks of 100% for 4 h and 80% for 8 h at approximately 4:00 and 7:00 a.m. correspondingly. A minimum of 20% of trouble rate is reached at 9:00 a.m. for 4 h and at 13:00 for 4 h, and there both remain until 16:00 when their accepted trouble rates increase again until they reach again their peaks in the next cycle. On the other hand, in the cases of 12 h and 16 h of trouble duration, the accepted trouble rate declines to 20% before 6:00, but rises again up to lower maximums than the other two cases until 16:00 as well. Additionally, in the cases of 16 h, 20 h and 24 h, the accepted trouble rate remains at 20% until 15:00. It then gradually increases, but shortly after it declines.

Based on Figs. 5 and 6, it could be said that, under duration when solar PV operates, the system is more vulnerable after the peak around 12:00 than before the peak, and also that the resilience of electricity power system for the battery trouble during periods when battery charges surplus power is more vulnerable compared with periods when battery is operated. This trend might be due to the difference in operational duration between solar PV and battery, that is: the battery operates throughout the day for charging during the day time and discharging during the night time while solar PV operates only during the day time. As long as the battery could ensure a continuous power supply until the start of solar PV operation even under the exposure of failures to some degree, the

hybrid renewable energy system could be self-sustained during the day time and the accepted trouble rate/duration could be accordingly extended. Besides that, the occurrence of disturbances on battery during day time directly leads to reduction of the amount of energy stored in the battery, which potentially cannot meet the requirement of energy demand at night.

It can be noted that the DI and RI curve presents the prediction of electricity resilience in the near future. The availability of these curves could be of use to implementers in examining countermeasures for the sudden failures of battery facilities and making wiser decisions in the customer services.

#### 4.2. Evaluation of system resilience

As outlined in section 2.1.3, the relationship between trouble duration, instant of trouble and trouble rate are the constituents of the quantitative analysis of system resilience proposed in this article. For each component, the integrals of the DI (trouble duration) and RI (trouble rate) curves outlined in the previous section are presented in Fig. 7.

From the plots in Fig. 7 it is observed that system resilience on a basis of DI curve decreases with increasing trouble rate and it is improved with increasing battery capacity. Under 0% of trouble rate, 576 points are obtained, which is a maximum value of

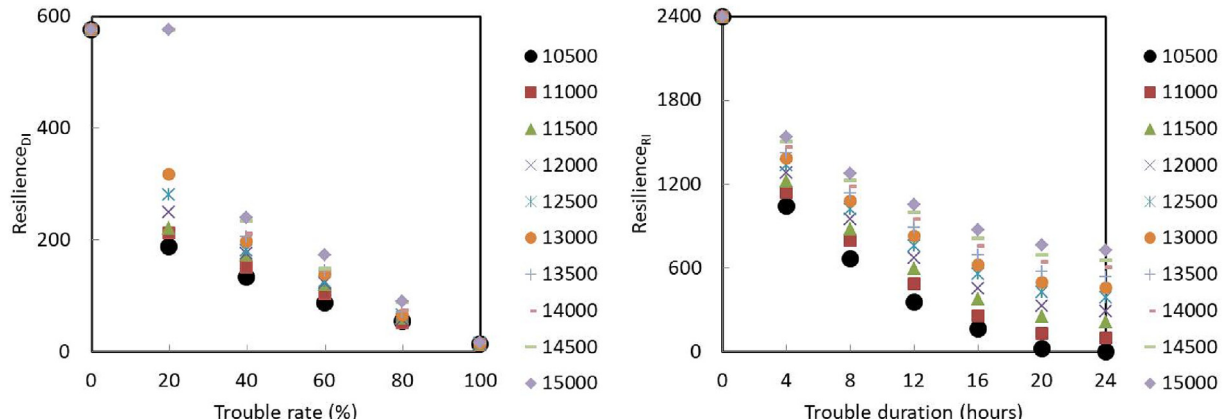


**Fig. 7.** Components of resilience in a sudden contingency of the battery system in a standalone power system.

$\text{resilience}_{\text{DI}}$  regardless with battery capacity. Meanwhile under 100% of trouble rate,  $\text{resilience}_{\text{DI}}$  is indicated in the range between 13.3 and 16.5 without any significant difference, which is a minimum value. In other word, the state of being exposed to the risk of 100% failures of battery operation presents merely 2% of maximum resilience in the power system compared with the case of no trouble on the facilities.

Each of battery capacities have a certain magnitude of trouble rate, under which the power disruption is not caused. Here it is named an accepted trouble rate, given in Fig. 8. Among the assessed battery capacity, the accepted trouble rate linearly increases with increasing battery capacity. Due to this trend, at 20% of trouble rate the power system with more than 13,500 Wh reaches the maximum resilience. Up to the accepted trouble rate,  $\text{resilience}_{\text{DI}}$  linearly increases with decreasing trouble rate.

From the plots in Fig. 7 it is observed that system resilience on a basis of RI curve decreases with increasing trouble duration and it is improved with increasing battery capacity. Under 0% of trouble rate, 2400 points are obtained, which is a maximum value of  $\text{resilience}_{\text{RI}}$  regardless with battery capacity. Meanwhile under 24 h of trouble duration,  $\text{resilience}_{\text{RI}}$  is indicated in the range between 0 and 724, which is a minimum value for each of battery capacities. Among the assessed battery capacity options, the minimum value of  $\text{resilience}_{\text{RI}}$  linearly increases. In other word, the state of being exposed to the risk of 24 h failures of battery operation presents 0% of maximum resilience in the power system compared with the case of no trouble on the facilities under 10500 Wh as the minimum battery capacity. On the other hand, it presents 30% of maximum resilience under 15000 Wh as the maximum battery capacity. In contrast to  $\text{resilience}_{\text{DI}}$ , it would appear that  $\text{resilience}_{\text{RI}}$  increases with decreasing trouble duration in an exponential manner.

By using Equations (5) and (7), the two indices for the overall resilience based on DI curve and RI curve are obtained. The result is presented in Fig. 9. Both indices almost linearly increase with increasing battery capacity. As for Overall resilience<sub>DI</sub>, the significant gap between 13,000 Wh and 13,500 Wh of battery capacity is caused by the differences of accepted trouble rate presented in Fig. 8.

The overall resilience<sub>DI</sub> is illustrated in the range 250–350, while the overall resilience<sub>RI</sub> is illustrated in the range 1000–1350. Given the maximum resilience<sub>DI</sub> and resilience<sub>RI</sub> are 576 and 2400, the normalized overall resilience<sub>DI</sub> and the normalized overall resilience<sub>RI</sub> are computed, presented in Table 2. Even for 10,500 Wh of required minimum battery capacity, more than 40% of maximum resilience could be contained in the developed method. And then, 15,000 Wh of battery capacity with 42.9% of capacity margin delivers 1.39 times in the overall resilience<sub>DI</sub> and 1.31 times in the overall resilience<sub>RI</sub> greater than 10,500 Wh of required minimum

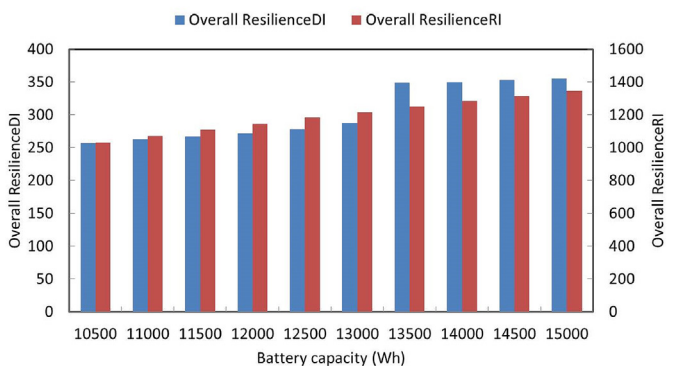


Fig. 9. Overall resilience of power system under the different battery capacity.

battery capacity. In other words, it could be possibly said that the incremental rate of power system resilience would be less than the incremental rate of capacity margin.

Setting the boundary of power system resilience would be useful to assist in designing the capacity size. The boundary might vary depending on the probability of disastrous event occurrence, battery component structure, the custom service quality, the installation location, and political and ideological implications. For example, given that the reserve margin in 2014 in Japan was 16.6% [87], 48.2% for the normalized overall resilience<sub>DI</sub> and 47.2% for the normalized overall resilience<sub>RI</sub> could be considered as a reference case of power system resilience in Japan. The reference case determined on a basis of current situation in each of countries would lead to the future resilience boundary covering the incremental risk of natural disasters arising from climate change.

The developed approach contributes to evaluating system resilience of electricity system dedicated for sudden disruptions of battery system under the various conditions of trouble rate, trouble duration on a basis of various instant of trouble. Meanwhile, the proposed algorithm could be further extended by taking into account additional factors. Firstly, this research focuses on the battery system troubles. On the other hand, renewable energy technologies including the solar PV also have possibilities of experiencing sudden disruptions. Inclusion of other energy sources in the system resilience analysis would cover the comprehensive ability of electricity system to remain self-sufficient after the occurrence of all types of sudden disruptions. In addition, the algorithm developed in this study is significantly associated with the system resilience and the concept of power adequacy is not covered. Integration of system resilience index in this research with adequacy index employing probabilistic approach would be of importance to comprehensively quantify the power reliability.

#### 4.3. Optimal storage technology in standalone hybrid renewable energy systems: results of DEA-based comparisons

Following the DEA-based procedure detailed in section 2.2, it was found that in general, larger battery capacities provide a better resilience score, being best performers those in the range of 13,500 to 15,000 Wh and worse ones those in 10,500–11,500 Wh.

Based on the results of DI and RI curves presented in Figs. 5 and 6, multiple cross sections represent diverse trouble rates and trouble durations within each figure, and such information had to be integrated to retrieve each resilience indicator introduced in the DEA model. To provide a wider perspective the integration had to consider diverse resilience index results; a range that started from a minimum rate, corresponding to the case where a largest area above the curve was found, and several mean values that

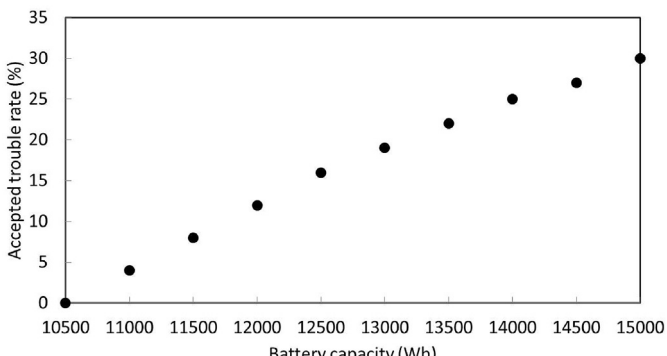


Fig. 8. Accepted trouble rate under the different battery capacity.

**Table 2**

Rate of overall resilience indices over the maximum resilience.

Battery capacity (Wh)	Normalized Overall Resilience <sub>DI</sub> (%)	Normalized Overall Resilience <sub>RI</sub> (%)
10,500	44.6	42.9
11,000	45.6	44.6
11,500	46.4	46.3
12,000	47.2	47.6
12,500	48.2	49.2
13,000	49.9	50.7
13,500	60.6	52.1
14,000	60.8	53.6
14,500	61.3	54.8
15,000	61.8	56.2

**Table 3**

Source data for DEA estimation.

Capacity [Wh]	Resilience index DI (trouble rate)					Resilience index RI (trouble duration)					Capita least[\$]
	Min	MM	GM	AM	RMS	Min	GM	AM	HM	RMS	
10,500	13.25	50.07	9841	175.37	256.77	0.01	57.08	662.43	0.01	1033.26	122 54
11,000	12.93	50.33	104.39	184.74	262.49	96.00	443.57	757.10	263.62	1070.14	12,390
11,500	1342	53.83	113.61	194.15	267.45	210.50	606.88	847.59	45.241	1110.23	12,527
12,000	13.04	52.33	115.17	199.10	271.85	291.00	703.67	910.94	563.97	1143.33	12,663
12,500	14.94	59.35	123.55	207.06	277.85	387.00	929.10	983.11	636.51	1133.04	12,800
13,000	14.77	59.99	130.22	218.33	237.26	460.20	333.79	1038.24	77.192	1216.91	12,936
13,500	15.56	64.05	148.76	264.73	349.28	532.00	954.07	1093.97	852.58	1250.31	13,073
14,000	16.10	66.07	151.46	266.41	350.00	604.00	1022.04	1143.61	933.00	1285.50	13,209
14,500	16.50	6942	160.02	273.27	353.23	653.00	1071.81	1183.97	985.23	1314.10	13,346
15,000	16.40	70.16	165.16	278.52	355.74	724.00	1132.12	1231.86	1084.08	1343.04	13,482

considered all the curves using different methods: Harmonic Mean (HM), Geometric Mean (GM), Arithmetic Mean (AM), and Root-Mean Square (RMS).<sup>1</sup> Table 3 summarizes the resilience indicators and Tables 4–6 the efficiency results of the DEA estimations.

From Table 4, we observe that resilience-to-cost efficiency of the system (considering both indices) mostly increase with a raise in storage capacity, albeit some noteworthy cases. First of all, systems with 11,000 and 12,000 Wh storage capacities seem to be slightly outperformed by the smaller 10,500 and 11,500 Wh type when focusing on the most critical resilience values (minimum and HM scores). The same could be said for the 14,500 Wh system, which could arguably be considered as good in performance as the 15,000 Wh type. Among systems in the mid-range of efficiency, the same holds for 12,500 Wh battery, which seems in fact a better performer than the 13,000 Wh one. Yet, we should keep in mind that all these assertions are based on the most critical values, because as the aggregation of resilience indices increase in magnitude from using alternative mean estimation methods, the correlation between efficiency and capacity is more clearly demonstrated.

Consistent with the general outcome, DEA models for each resilience index with cost assessed separately (Tables 5 and 6) support the overall finding. Progressive increase in the efficiency correlates with larger capacity. Yet, solely looking at each resilience indicator does not favour the cases of some smaller-capacity batteries outperforming their consecutive larger one, as attested and explained above through the analysis of the DEA model considering both indicators.

In sum, through the DEA outcomes in this section we can conclude that as a general rule larger battery capacities provide higher resilience, but for the most critical situation some particular types can be as or even somewhat more efficient than the immediate larger types in the list considering both trouble rate and trouble duration.

**Table 4**DEA results (overall resilience<sub>DI</sub>, overall resilience<sub>RI</sub>, and capital cost).

capacity (Wh)	Min	HM	GM	AM	RMS
10,500	87.5%	78.5%	65.6%	69.3%	84.1%
11,000	84.4%	78.1%	68.8%	72.2%	86.4%
11,500	86.7%	82.6%	74.0%	75.0%	88.6%
12,000	83.3%	80.2%	74.2%	78.7%	90.3%
12,500	94.4%	89.1%	78.8%	84.1%	92.4%
13,000	92.3%	89.1%	82.2%	87.8%	94.1%
13,500	96.3%	94.2%	92.9%	98.0%	100.0%
14,000	98.6%	96.1%	93.6%	97.6%	99.7%
14,500	100.0%	100.0%	97.9%	99.1%	99.9%
15,000	100.0%	100.0%	100.0%	100.0%	100.0%

**Table 5**DEA results (overall resilience<sub>DI</sub> and capital cost).

capacity (Wh)	Min	HM	GM	AM	RMS
10,500	87.5%	78.5%	65.6%	69.3%	78.4%
11,000	84.4%	78.1%	68.8%	72.2%	79.3%
11,500	86.7%	82.6%	74.0%	75.0%	79.9%
12,000	83.3%	80.2%	74.2%	76.1%	80.3%
12,500	94.4%	89.1%	78.8%	78.3%	81.2%
13,000	92.3%	89.1%	82.2%	81.7%	83.1%
13,500	96.3%	94.2%	92.9%	98.0%	100.0%
14,000	98.6%	96.1%	93.6%	97.6%	99.2%
14,500	100.0%	100.0%	97.9%	99.1%	99.1%
15,000	98.4%	100.0%	100.0%	100.0%	98.8%

**Table 6**DEA results (overall resilience<sub>RI</sub> and capital cost).

capacity (Wh)	Min	HM	GM	AM	RMS
10,500	0.0%	0.0%	5.5%	59.2%	84.1%
11,000	14.4%	27.2%	42.6%	66.9%	86.4%
11,500	31.3%	46.2%	57.7%	74.1%	88.6%
12,000	42.8%	57.0%	66.2%	78.7%	90.3%
12,500	56.3%	68.6%	75.3%	84.1%	92.4%
13,000	66.2%	76.3%	81.4%	87.8%	94.1%
13,500	75.8%	83.4%	86.9%	91.3%	95.7%
14,000	85.1%	90.1%	92.1%	94.8%	97.3%
14,500	91.1%	94.4%	95.6%	97.1%	98.5%
15,000	100.0%	100.0%	100.0%	100.0%	100.0%

<sup>1</sup> Details on the means estimation methods can be found in Ref. [88].

## 5. Conclusion

This research first proposed the methodology of analyzing system resilience in response to sudden disruptions of battery system from the three major parameters: magnitude, duration and instant of sudden battery system failure. System resilience was defined as the ability of electricity system to remain self-sufficient after the occurrence of sudden disruptions. The relationship between trouble duration and instant of trouble and trouble rate was identified by changing the three major parameters associated with battery trouble. And then, the system resilience index dedicated for the sudden disruption of battery trouble was proposed in a quantitative way.

It was discovered that system resilience declines with increasing trouble rate and trouble duration in the downward-convex exponential manner. In addition, under duration when solar PV operates, system resilience is more vulnerable after the peak around 12:00 than before the peak. Furthermore, the resilience of electricity power system for the battery trouble during periods when battery charges surplus power is more vulnerable compared with periods when battery is operated.

Through a DEA-based comparison of storage technology, we can conclude that in general larger storage capacity provides higher resilience, but in the most critical situations some particular types can be as or even marginally more resilient than the immediate larger types, considering both trouble rate and trouble duration.

The methodology developed in this study could be considered as a simplified assessment at this stage just assuming an imaginary dynamic behavior in sudden disturbances. Due to the complexity of computational modelling and lack of sufficient data as current drawbacks of analyzing dynamic behavior, the conceivable advantage of this study would be to perform with the use of simplified concept the security and resilience in the hybrid renewable energy system which has not extensively been addressed so far. Meanwhile, more practical perspectives are left out such as the technical limitation and control management, interactions between solar PV, battery and intermittent uncertainties of solar radiation and the real and technical dynamic change of power system. The integration of these technical perspectives in the developed methodology would assist in presenting more practical framework for addressing the issue of sudden disturbances.

## Appendix A. Supplementary data

Supplementary data to this article can be found online at <https://doi.org/10.1016/j.energy.2020.117133>.

## References

- [1] Ajan CW, Ahmed SS, AHB, Taha F, Mohd Zin AAB. On the policy of photovoltaic and diesel generation mix for an off-grid site: East Malaysian perspectives. *Sol Energy* 2003;74:453–67. 2003.
- [2] World Bank. "Access to electricity," global electrification database, world bank. web site, <http://data.worldbank.org/indicator/EG.ELC.ACCS.ZS?end=2012&start=1990>. [Accessed 7 December 2016].
- [3] Jakhrani AQ, Othman AK, Rigit ARH, Samo SR. Assessment of solar and wind energy resources at five typical locations in Sarawak. *J Energy Environ* 2012;4(1):1–6.
- [4] Voss K, Musall E, Lichtmeß M. From low energy to net zero energy building: status and perspectives. *Green Build* 2011;6:46–57.
- [5] Deng S, Wang RZ, Dai YJ. How to evaluate performance of net zero energy building - a literature research. *Energy* 2014;1–16.
- [6] Kosai S, Tan C. Quantitative analysis on a zero energy building performance from energy trilemma perspective. *Sustain Cities Soc* 2017;32:130–41.
- [7] Crawley D, Pless S, Torcellini P. Getting to net zero. *ASHRAE J* 2009;51(9):18–25.
- [8] Vale B, Vale R. The new autonomous house: design and planning for sustainability. Thames & Hudson Ltd; 2002.
- [9] Feist W. Life-cycle energy analysis: comparison of low-energy house, passive house and self-sufficient house. In: Proceedings of the international symposium of CIB W67; 1997. Vienna, Austria.
- [10] Saxena N, Hussain I, Singh B, Vyas AL. Implementation of a grid-integrated PV-battery system for residential and electrical vehicle applications. *IEEE Trans Ind Electron* 2018;65(8):6592–601.
- [11] Arbabzadeh M, Johnson JX, Keoleian GA, Rasmussen PG, Thompson LT. Twelve principles for green energy storage in grid applications. *Environ Sci Technol* 2016;50(2):1046–55.
- [12] Allan R. Power system reliability assessment-a conceptual and historical review. *Reliab Eng Syst Saf* 1994;46(1):3–13.
- [13] North American Electric Reliability Council (NERC). Glossary of terms used in NERC reliability standards. web site, [www.nerc.com/files/glossary\\_of\\_terms.pdf](http://www.nerc.com/files/glossary_of_terms.pdf). [Accessed 1 March 2017].
- [14] Yang HX, Lu L, Zhou W. A novel optimization sizing model for hybrid solar-wind power generation system. *Sol Energy* 2007;81(1):76–84.
- [15] Diaf S, Diaf D, Belhamel M, Haddadi M, Louche A. A methodology or optimal sizing of autonomous hybrid PV/wind system. *Energy Pol* 2007;35(11):5708–18.
- [16] Semaoui S, Arab AH, Bacha S, Azoui B. Optimal sizing of a stand-alone photovoltaic system with energy management in isolated areas. *Energy Procedia* 2013;36:358–68.
- [17] Cho JH, Chun MG, Hong WP. Structure optimization of stand-alone renewable power systems based on multi object function. *Energies* 2016;9(8):649.
- [18] Das BK, Al-Abdeli YM, Kothapalli G. Optimisation of stand-alone hybrid energy systems supplemented by combustion-based prime movers. *Appl Energy* 2017;196:18–33.
- [19] Vergara PP, Rey JM, da Silva LCP, Ordóñez G. Comparative analysis of design criteria for hybrid photovoltaic/wind/battery systems. *IET Renew Power Gener* 2017;11(3):253–61.
- [20] Maleki A, Pourfayaz F, Hafeznia H, Rosen MA. A novel framework for optimal photovoltaic size and location in remote areas using a hybrid method: a case study of eastern Iran. *Energy Convers Manag* 2017;153:129–43.
- [21] Cabral CVT, Filho DO, Diniz ASAC, Martins JH, Toledo OM, de Vilhena BL, Neto M. A stochastic method for stand-alone photovoltaic system sizing. *Sol Energy* 2010;84(9):1628–36.
- [22] Arun P, Banerjee R, Bandyopadhyay S. Optimum sizing of photovoltaic battery systems incorporating uncertainty through design space approach. *Sol Energy* 2009;83(7):1013–25.
- [23] Roy A, Kedare SB, Bandyopadhyay S. Optimum sizing of wind-battery systems incorporating resource uncertainty. *Appl Energy* 2010;87(8):2712–27.
- [24] Jakhrani AQ, Othman A-K, Rigit ARH, Samo SR, Kamboh SA. A novel analytical model for optimal sizing of standalone photovoltaic systems. *Energy* 2012;46(1):675–82.
- [25] Chen HC. Optimum capacity determination of stand-alone hybrid generation system considering cost and reliability. *Appl Energy* 2013;103:155–64.
- [26] Agarwal N, Kumar A, Varun. Optimization of grid independent hybrid PV-diesel-battery system for power generation in remote-villages of Uttar Pradesh, India. *Energy Sustain Dev* 2013;17(3):210–9.
- [27] Ma G, Xu GC, Chen YX, Ju R. Multi-objective optimal configuration method for a standalone wind-solar-battery hybrid power system. *IET Renew Power Gener* 2017;11(1):194–202.
- [28] Muhsen DH, Khatib T, Abdulabbas TE. Sizing of a standalone photovoltaic water pumping system using hybrid multi-criteria decision making methods. *Sol Energy* 2018;159:1003–15.
- [29] Rajanna S, Saini RP. Modeling of integrated renewable energy system for electrification of a remote area in India. *Renew Energy* 2016;90:175–87.
- [30] Alinejad B, Fotuhi-firuzabad M, Parvania M. Composite system well-being analysis using sequential Monte Carlo simulation and fuzzy algorithm. *IU-J Electr Electron Eng* 2013;13(1):1575–80.
- [31] Suchitra D, Jegatheesan R, Deepika TJ. Optimal design of hybrid power generation system and its integration in the distribution network. *Int J Electr Power Energy Syst* 2016;82:136–49.
- [32] Ramli MAM, Bouchekara HREH, Alghamdi AS. Optimal sizing of PV/wind/diesel hybrid microgrid system using multi-objective self-adaptive differential evolution algorithm. *Renew Energy* 2018;121:400–11.
- [33] Novoa C, Jin TD. Reliability centered planning for distributed generation considering wind power volatility. *Elec Power Syst Res* 2011;81(8):1654–61.
- [34] Zolfaghari S, Riahy GH, Abedi M, Golshannavaz S. Optimal wind energy penetration in power systems: an approach based on spatial distribution of wind speed. *Energy Convers Manag* 2016;118:387–98.
- [35] Gangwar S, Bhanja D, Biswas A. Cost, reliability, and sensitivity of a stand-alone hybrid renewable energy system-A case study on a lecture building with low load factor. *J Renew Sustain Energy* 2015;7(1):013109.
- [36] Ayop R, Isa NM, Tan CW. Components sizing of photovoltaic stand-alone system based on loss of power supply probability. *Renew Sustain Energy Rev* 2018;81:2731–43.
- [37] Hu H, Augenbroe G. A stochastic model based energy management system for off-grid solar houses. *Build Environ* 2012;50:90–103.
- [38] Benidris M, Mitra J, Singh C. Integrated evaluation of reliability and stability of power systems. *IEEE Trans Power Syst* 2017;32(5):4131–9.
- [39] Takahata AY, dos Santos MG, Taranto GN, Schilling MT. Computational framework combining static and transient power system security evaluation using uncertainties. *Int J Electr Power Energy Syst* 2015;71:151–9.
- [40] Panteli M, Pierluigi M. Influence of extreme weather and climate change on the resilience of power systems: impacts and possible mitigation strategies. *Elec Power Syst Res* 2015;127:259–70.

- [41] Kosai S, Unesaki H. Quantitative analysis on the impact of nuclear energy supply disruption on electricity supply security. *Appl Energy* 2018;208: 1198–207.
- [42] Rocchetta R, Patelli E. Assessment of power grid vulnerabilities accounting for stochastic loads and model imprecision. *Int J Electr Power Energy Syst* 2018;98:219–32.
- [43] Roach M. Community power and fleet microgrids: meeting climate goals enhancing system resilience and stimulating local economic development. *IEEE Electrification Magazine* 2014;2(1):40–53.
- [44] Simonov M. Dynamic partitioning of DC microgrid in resilient clusters using event-driven approach. *IEEE Trans Smart Grid* 2014;5(5):2618–25.
- [45] Zare-Bahramabadi M, Abbaspour A, Fotuhi-Firuzabad M, Moeini-Aghaie M. Resilience-based framework for switch placement problem in power distribution systems. *IET Gener, Transm Distrib* 2018;12(5):1223–30.
- [46] Liu XD, Shahidehpour M, Cao YJ, Li Z, Tian W. Risk assessment in extreme events considering the reliability of protection systems. *IEEE Trans Smart Grid* 2015;6(2):1073–81.
- [47] Li GF, Zhang P, Luh PB, Li WY, Bie ZH, Serna C, Zhao ZB. Risk analysis for distribution systems in the Northeast U.S. under wind storms. *IEEE Trans Power Syst* 2014;29(2):889–98.
- [48] Panteli M, Pickering C, Wilkinson S, Dawson R, Mancarella P. Power system resilience to extreme weather: fragility modeling, probabilistic impact assessment, and adaptation measures. *IEEE Trans Power Syst* 2017;32(5): 3747–57.
- [49] Chen C, Wang J, Qiu F, Zhao DB. Resilient distribution system by microgrids formation after natural disasters. *IEEE Trans Smart Grid* 2016;7(2):958–66.
- [50] Wang Z, Wang J. Self-healing resilient distribution systems based on sectionalization into microgrids. *IEEE Trans Power Syst* 2015;30(6):3139–49.
- [51] Nikmehr N, Sajad N. Optimal operation of distributed generations in microgrids under uncertainties in load and renewable power generation using heuristic algorithm. *IET Renew Power Gener* 2015;9(8):982–90.
- [52] Panteli M, Trakas DN, Mancarella P, Hatziargyriou ND. Boosting the power grid resilience to extreme weather events using defensive islanding. *IEEE Trans Smart Grid* 2016;7(6):2913–22.
- [53] Espiritu JF, Coit DW, Prakash U. Component criticality importance measures for the power industry. *Elec Power Syst Res* 2007;77(5–6):407–20.
- [54] Cadini F, Agliardi GL, Zio E. A modeling and simulation framework for the reliability/availability assessment of a power transmission grid subject to cascading failures under extreme weather conditions. *Appl Energy* 2017;185: 267–79.
- [55] Moradkhani A, Haghifam MR, Mohammadzadeh M. Failure rate estimation of overhead electric distribution lines considering data deficiency and population variability. *Int Trans Electr Energy Syst* 2015;25(8):1452–65.
- [56] Chaudry M, Wu JZ, Jenkins N. A sequential Monte Carlo model of the combined GB gas and electricity network. *Energy Pol* 2013;62:473–83.
- [57] Javadian SAM, Haghifam MR, Fotuhi Firoozabad M, Bathaei SMT. Analysis of protection system's risk in distribution networks with DG. *Int J Electr Power Energy Syst* 2013;44(1):688–95.
- [58] Kosai S, Tan CK, Yamasue E. Evaluating power reliability dedicated for sudden disruptions: its application to determine capacity size on a basis of energy security. *Sustainability* 2018;10(6):2059.
- [59] Kosai S, Yamasue E. Cost-security analysis dedicated for the off-grid electricity system. *Renew Energy* 2017. <https://doi.org/10.1016/j.renene.2017.09.024>.
- [60] Kosai S. Dynamic vulnerability in standalone hybrid renewable energy system. *Energy Convers Manag* 2019;180:258–68.
- [61] Nguyen CP, Flueck AJ. Agent based restoration with distributed energy storage support in smart grids. *IEEE Trans Smart Grid* 2012;3(2):1029–38.
- [62] Shankar R, Chatterjee K, Bhushan R. Impact of energy storage system on load frequency control for diverse sources of interconnected power system in deregulated power environment. *Int J Electr Power Energy Syst* 2016;79: 11–26.
- [63] Gouveia C, Moreira CL, Lopes JAP, Varajao D, Araujo RE. Microgrid service restoration: the role of plugged-in electric vehicles. *IEEE Ind Electron Mag* 2013;7(4):6–41.
- [64] Stirling A. From sustainability, through diversity to transformation: towards more reflexive governance of technological vulnerability. In: Hommels A, Mesman J, Bijker W, editors. *Vulnerability in technological cultures: new directions in research and governance*. Inside technology. Cambridge, MA: MIT Press; 2014.
- [65] Winzer C. Conceptualizing energy security. *Energy Pol* 2012;46:36–48.
- [66] Kundur P, Paserba J, Ajjarapu V, Andersson G, Bose A, Canizares C, Hatziargyriou N, Hill D, Stankovic A, Taylor C, Van Curseum T, Vittal V. Definition and classification of power system stability. *IEEE Trans Power Syst* 2004;19(3):1387–401.
- [67] Cooper WW, Seiford LM, Tone K. Data envelopment analysis. A comprehensive text with models, applications, references and DEA-Solver software. second ed. New York: Springer; 2007.
- [68] Bilal BO, Sambou V, Ndiaye P, Kb C, Ndongo M. Optimal design of a hybrid solar-wind-battery system using the minimization of the annualized cost of the system and the minimization of the loss of power supply probability (LSP). *Renew Energy* 2010;35:2388–90.
- [69] Dufo-Lpez R, Bernal-Agustin JL, Mendoza F. Design and economical analysis of hybrid pv wind systems connected to the grid for the intermittent production of hydrogen. *Energy Pol* 2009;37:3082–95.
- [70] Charnes A, Cooper WW, Rhodes E. Measuring the efficiency of decision making units. *Eur J Oper Res* 1978;2(6):429–44.
- [71] Cullinane K, Wang T, Song DW, Ji P. The technical efficiency of container ports: comparing data envelopment analysis and stochastic frontier analysis. *Transport Res Pol Pract* 2006;40(4):354–74.
- [72] Stewart D. Habitat and ecology: the cohousing experiment in the United States. *Rev Fr Études Am* 2002;94:113–27.
- [73] Ministry of Economy, Trade and Industry (METI). "ZEH load map. available at: <http://www.meti.go.jp/press/2015/12/20151217003/20151217003-1.pdf>. [Accessed 27 May 2015].
- [74] Wolstenholme E. *System Enquiry. A system dynamics approach*. Chichester: John Wiley and Sons.; 1990.
- [75] Kosai S, Rahim NA. Energy mix with the vulnerability of nuclear power utilization. In: IET conference publications, volume 2016, issue CP688, proceeding in 4th IET international conference on clean energy and technology CEAT 2016; 2016. p. 1–7. <https://doi.org/10.1049/cp.2016.1332>. 14–15 November 2016, Kuala Lumpur, Malaysia.
- [76] Richardson GP. *System dynamics*. In: *Encyclopedia of operations research and management science*. Kluwer Academic Publishers; 2011.
- [77] Senge P. *The Fifth Discipline: the art and practice of learning organization*. Random House Business; 1990. p. 424.
- [78] Lempert R, Popper S, Banks S. Shaping the next one hundred years: new methods for quantitative, long-term policy analysis," RAND report MR-1626. 2003.
- [79] Post HN, Thomas MG. Photovoltaic systems for current and future applications. *Sol Energy* 1998;41(5):456–73.
- [80] Yano Research Institute Ltd. Next generation homes and related equipment market 2019. Yano Research Institute Ltd.; 2019. p. C60125700. in japanese.
- [81] Ministry of Economy, Trade and Industry (METI). "peak demand in summer. <http://www.meti.go.jp/setsuden/20110513taisaku/16.pdf>. [Accessed 29 August 2015].
- [82] New Energy and Industrial Technology Development Organization (NEDO). NEDO irradiation data base. available at: <http://app0.infoc.nedo.go.jp/metpv/metpv.html>. [Accessed 8 July 2016].
- [83] Skandalos N, Karamanis D. PV glazing technologies. *Renew Sustain Energy Rev* 2015;49:306–22.
- [84] Chen H, Cong T, Yang W, Tan C, Li Y, Ding Y. Progress in electrical energy storage system: a critical review. *Progress in Nature Science* 2009;19: 291–312.
- [85] Curry C. Lithium-ion battery costs and market. available at: <https://data.bloomberg.com/bnef/sites/14/2017/07/BNEF-Lithium-ion-battery-costs-and-market.pdf>. [Accessed 16 August 2018].
- [86] National Renewable Energy Laboratory, U.S. Solar photovoltaic system cost benchmark. National Renewable Energy Laboratory; 2017.
- [87] Federation of Electric Power Companies of Japan. The electric power industry in Japan 2018. available at: [https://www.jepic.or.jp/en/data/japan\\_data.pdf](https://www.jepic.or.jp/en/data/japan_data.pdf). [Accessed 7 August 2018].
- [88] Bullen PS, Mitrovic DS, Vasic M. *Means and their inequalities*, vol. 31. Springer Science & Business Media.; 2013.
- [89] Kosai S, Unesaki H. Short-term vs long-term reliance: Development of a novel approach for diversity of fuels for electricity in energy security. *Applied Energy* 2020;262(114520). <https://doi.org/10.1016/j.apenergy.2020.114520>.